JOURNAL OF NEUROTRAUMA 29:1691–1703 (May 20, 2012)

DOI: 10.1089/neu.2011.1857

Traumatic Neuroma in Continuity Injury Model in Rodents

Jacob Daniel de Villiers Alant,[1] Stephen William Peter Kemp,[1] Kathleen Joy Ong Lopez Khu,[2] Ranjan Kumar,[3] Aubrey A. Webb,[1] and Rajiv Midha[1]

Abstract

Traumatic neuroma in continuity (NIC) results in profound neurological deficits, and its management poses the most challenging problem to peripheral nerve surgeons today. The absence of a clinically relevant experimental model continues to handicap our ability to investigate ways of better diagnosis and treatment for these disabling injuries. Various injury techniques were tested on Lewis rat sciatic nerves. Optimal experimental injuries that consistently resulted in NIC combined both intense focal compression and traction forces. Nerves were harvested at 0, 5, 13, 21, and 65 days for histological examination. Skilled locomotion and ground reaction force (GRF) analysis were performed up to 9 weeks on the experimental ($n = 6$) and crush-control injuries ($n = 5$). Focal widening, disruption of endoneurium and perineurium with aberrant intra- and extrafascicular axonal regeneration and progressive fibrosis was consistently demonstrated in 14 of 14 nerves with refined experimental injuries. At 8 weeks, experimental animals displayed a significantly greater slip ratio in both skilled locomotor assessments, compared to nerve crush animals ($p < 0.01$). GRFs of the crush- injured animals showed earlier improvement compared to the experimental animals, whose overall GRF patterns failed to recover as well as the crush group. We have demonstrated histological features and poor functional recovery consistent with NIC formation in a rat model. The injury mechanism employed combines traction and compression forces akin to the physical forces at play in clinical nerve injuries. This model may serve as a tool to help diagnose this injury earlier and to develop intervention strategies to improve patient outcomes.

Key words: locomotion; nerve injury; nerve regeneration; neuroma; Sunderland grade 4 injury

Introduction

The spectrum of peripheral nerve injuries forms a continuum. Seddon first introduced the popular 3-tiered classification of neurapraxia, axonotmesis, and neurotmesis (Seddon, 1943). Sunderland further expanded on this classification, introducing a 5-tiered system to depict progressive severity with anatomical and functional correlates (Sunderland, 1951). Grade 1 (neurapraxia) and 2 (limited to axonotmesis) injuries usually recover with no or insignificant functional deficits within a few weeks to months, respectively. Injuries that are most difficult to manage clinically are the often mixed grade 3 (endoneurial disruption) and 4 (perineurial disruption) lesions, where spontaneous functional recovery is limited or absent, giving rise to a Sunderland "mixed lesion" or neuroma in continuity (NIC; Mackinnon, 1989). Grade 5 (nerve transection) injuries are usually associated with lacerating wounds and are therefore recognized and repaired early.

It remains a clinical challenge to identify the injuries early that would result in NIC. By the time that it is clear that functional recovery is minimal, nerve regeneration and the recovery potential of the denervated end-organ are significantly handicapped (Fu and Gordon 1995a,b; Furey et al., 2007). Delayed repair strategies (e.g., neuroma excision with graft repair and/or neurotization) are then employed with varied and often limited success. Experimental models play a central role in unraveling the intricate mechanisms of nerve regeneration that cannot be studied in our patients. Several animal models for the study of nerve regeneration after injuries have been developed, reproducing mostly grade 2 (crush) and 5 (transection) lesions, but also features of grade 3 and 4 injuries were demonstrated with electrothermal forces (Hnatuk et al., 1998; Moradzadeh et al., 2010; Tos et al., 2009). To our knowledge, no rodent or other animal model has yet been refined or validated to reproduce *in vivo* grade 3 and 4 injuries by employing physical forces akin to those responsible for the majority of injuries encountered clinically. A simple

[1]Department of Clinical Neurosciences, Hotchkiss Brain Institute, University of Calgary, Calgary, Alberta, Canada.
[2]Division of Neurosurgery, Department of Neurosciences, Philippine General Hospital, Ermita, Manila, Philippines.
[3]Department of Neuroscience, University of Calgary, Calgary, Alberta, Canada.

small-animal model for NIC would be invaluable to make this elusive and devastating injury amenable to basic science research.

Because of the resilience and very effective/efficient peripheral nerve regeneration observed in rodents, it is challenging to recreate the histological features seen in human NIC. Human traumatic NIC is characterized by aberrant intra- and extrafascicular axonal regeneration and scar formation within an unsevered injured nerve, resulting in impaired and erroneous end-organ reinnervation (Burger et al., 2002; Chen et al., 2008; Sunderland, 1951). Clinically prototypical NIC is encountered in brachial plexus injuries, the incidence of which approaches 5% among motorcycle and snowmobile accident victims (Midha, 1997). Tandem lesions with or without nerve root avulsion are not uncommon. Traction forces applied to the brachial plexus, tethered at various locations, are thought to play a major role in closed plexus injuries (Midha, 2008). Degrees of direct compression of the nerves by the applied blunt forces and adjacent structures complicate this injury mechanism.

Our goal was to develop a practical rodent model for focal traumatic NIC by using clinically relevant forces to reproduce the characteristic histological features, supported by demonstrable functional deficits. We compare the histological features and behavioral effects of our preliminary sciatic nerve NIC injury model to the well established but less severe experimental sciatic nerve crush injury in this report.

Methods

Animals

Adult male Lewis rats (28 in total; Table 1), weighing approximately 250–300 g (Charles River Laboratories International Inc., St. Constant, Quebec, Canada), were used in this study, with all *in vivo* interventions carried out under inhalation anesthetic (isoflurane; Halocarbon Laboratories, River Edge, NJ). Animal numbers and *in vivo* experiments were minimized by performing preliminary experiments (*ex vivo*) on freshly harvested sciatic nerves of animals sacrificed for other research purposes. All experimental animals were maintained in a temperature- and humidity-controlled environment, and were fed standard rat chow (Purina, Mississauga, Ontario, Canada) restricted to 4 pellets/animal/day and water *ad libitum*, with a 12:12-h light-dark cycle. All surgical procedures were carried out using standard microsurgical and aseptic technique and an operating microscope (Wild M651; Wild Leitz, Willowdale, Ontario, Canada). Buprenorphine (0.03 mg/kg) subcutaneous injection followed by jello with buprenorphine was used for postoperative analgesia. The surgical procedures were well tolerated by all animals, with no complications observed. The animals were sacrificed at study termination, under deep inhalation anesthesia, with intracardiac Euthanol (Bimeda-MTC, Cambridge, Ontario, Canada). The protocol was approved by the University of Calgary Animal Care Committee and adhered strictly to the Canadian Council on Animal Care guidelines.

Specimen processing and microscopy

The harvested nerves were post-fixed in 4% paraformaldehyde overnight, cryoprotected in 30% sucrose/phosphate-buffered saline solution, and then embedded in embedding compound. Proper orientation (straight and proximal-distal) of the harvested nerves was ensured. The microtome (Leica CM1900; Leica Microsystems Inc., Richmond Hill, Ontario, Canada) was set to 8 μm, and serial longitudinal sections were cut at -22°C and mounted onto Superfrost Plus slides (Fisher Scientific, Ottawa, Ontario, Canada). Hematoxylin and eosin (H&E) and Masson's trichrome (Sigma-Aldrich Canada Ltd., Oakville, Ontario, Canada) stains were used, in addition to neurofilament (NF200, 1:600 dilution; Sigma-Aldrich), and laminin (α-1 E3-1, 1:50 dilution; Santa Cruz Biotechnology Inc., Santa Cruz, CA) immunofluorescent stains were used according to standard supplier protocols. Selected sections were double stained for laminin and neurofilament. Sections were examined with a fluorescence microscope (Olympus BX51; Olympus, Center Valley, PA) using the appropriate filters. Photomicrographs were taken of the injury zones at different magnifications for comparison before significant photo bleaching could occur.

Injury methodology

Ex vivo experiments suggested that intense compression with or without traction may result in the desired degree of injury. Four *in vivo* injury combinations were macroscopically and microscopically evaluated at 5- and 13-day time points to help select the better force combination (Table 1). Simple 30-sec jeweler's forceps (Dumont #5; Fine Surgical Tools Inc., North Vancouver, B.C., Canada) crush with and without 50 g traction (as histological controls), and 3-sec malleus nipper (Stotz N1430; Bausch & Lomb, Rochester, NY) injuries, with and without 50 g traction were compared. Sciatic nerves were exposed from where they emerge from the sciatic notch to the popliteal fossa (± 20 mm) through a longitudinal lateral thigh incision, splitting the biceps femoris muscle. A mesoneurial 6-0 Prolene suture was placed proximal to the sciatic

Table 1. The Investigational Groups and Numbers Analyzed for Histology at Various Time Points

Injury	(n)	*Day 5*	*13*	*21*	*65*[a]	*Main histology findings*
Simple crush (control)	7	1	1		5	No EN or PN disruption
Crush with 50 g traction	2	1	1			Minimal EN, PN disruption
MN compression (no traction)	5	4	1			Minimal EN, PN disruption
MN compression with 50 g traction (experimental neuroma in continuity)	14	5	1	2	6	Uniform EN, PN disruption

[a]Histology from rats allocated to the behavioral experiment.

The malleus nipper with 50 g traction experiments were the only ones to consistently demonstrate histological features concordant with neuroma in continuity.

EN, endoneurium; PN, perineurium; MN, malleus nipper.

trifurcation, just distal to the middle of the exposed nerve segment. A small unnamed cutaneous branch, perforating the biceps femoris muscle together with small vessels, separates from the sciatic common epineurium at this site, and was severed to mobilize the sciatic nerve circumferentially.

We selected a simple pen-style 100×1 g traction spring scale (AMW-PEN100; American Weigh Sales Inc., Norcross, GA) to apply the traction force, after it was decided that 50 g traction was to be used for the experimental model. The clamp was removed from the end to leave a conveniently-sized hook for placement around the nerve (Fig. 1). A 50-g calibration weight was used to confirm accuracy of the traction scale. The traction was applied perpendicular to the native nerve course, with the hook of the scale placed at the midpoint of the mobilized nerve. This roughly distributes traction vectors equally between the proximal and distal segments without adding a significant additional focal injury by not requiring a firm fixation point onto the nerve. The compressing instrument was placed in position along with (distal to) the hook of the traction scale (when used; Fig. 1). It took only a few seconds to pull on the traction scale with one hand up to the 50-g point, and then the same surgeon inflicted the focal injury with the other hand. The injuries were made immediately distal to the mesoneurial suture, where fascicular separation was evident within the common epineurium of the sciatic nerve. Traction (when used) was maintained for 30 sec in combination with the jeweler's forceps crush, and only for 3 sec with the malleus nipper. We paid attention not to overcompress the jeweler's forceps to avoid splaying of the forceps tips.

Malleus nipper compression was applied using maximal closing force. We used the touching of the handle (proximal) ends as the fixed endpoint for maximal force application. This ensures a relatively consistent compression force that cannot be exceeded. The approximate maximal closing force with this method was measured using a thin load cell (Flexiforce medium B201 with ELF™; Tekscan Inc., South Boston, MA). The sciatic nerve flattens transversely upon compression to contact approximately 2.22 mm of the blade of the compressive instrument. The surface area of 2.22 mm of the blades (centered 2 mm from the distal end), as imprinted on a thin plastic film with maximal instrument closure as described, was measured and used to calculate the approximate maximal

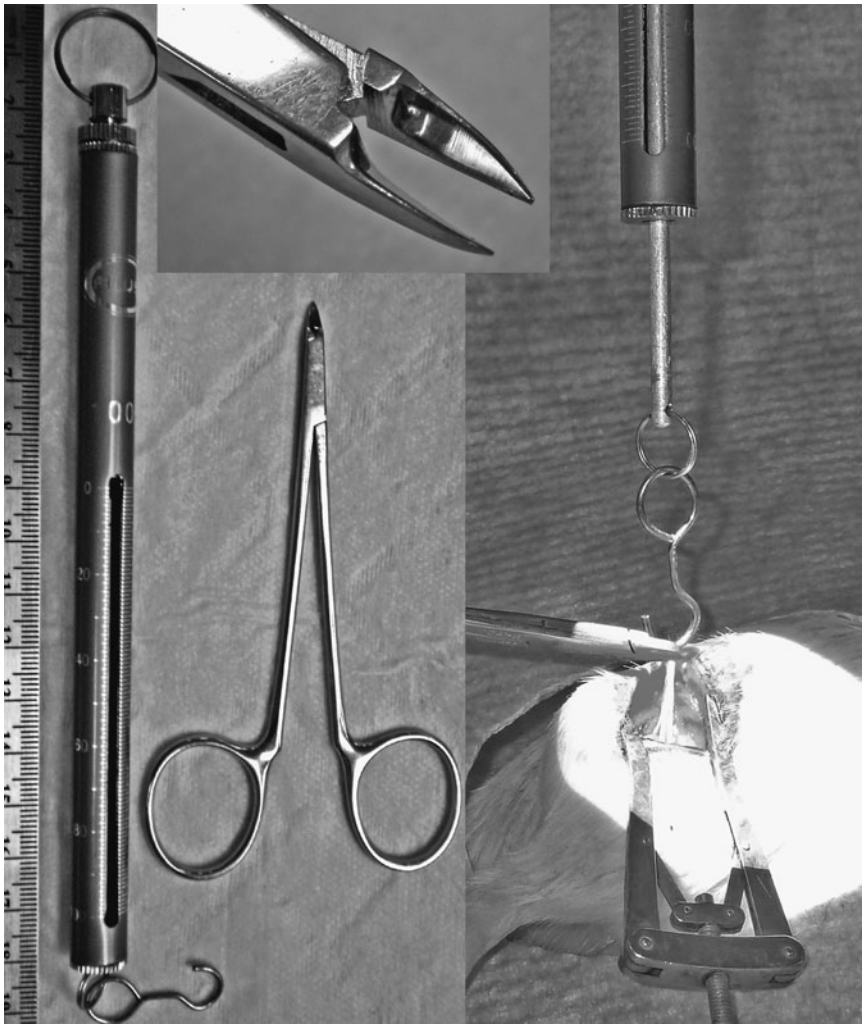

FIG. 1. The 100×1g spring scale is hooked around the mobilized sciatic nerve and 50 g of traction is applied orthogonal to the native nerve course. With the malleus nipper, intense focused compression is applied for 3 sec before the traction is released. The top inset shows the malleus nipper tip detail.

pressure exerted by the blades [force (N)/surface area (m^2) = pressure (Pa)]. For reference, this was also measured for the distal 2.22 mm of the no. 5 jeweler's forceps with the same technique. Six consecutive maximal force measurements were used to calculate the average pressures.

For behavioral outcomes and additional histology, 11 animals were randomized into experimental ($n = 6$) and simple crush injury ($n = 5$) groups (Table 1). The refined experimental injuries were inflicted to the right sciatic nerves, with the same malleus nipper (3 sec maximal compression and 50 g traction). Crush injuries (30 sec with jeweler's forceps without traction) were inflicted using similar exposure, mobilization, and marking techniques, and wound closure.

Injured sciatic nerves were carefully exposed and minimally manipulated for mobilization with the aid of a microscope at 5, 13, 21, and 65 days for *in situ* pictures and harvesting of the ± 20-mm marked nerve segment (10 mm proximal and distal to the mesoneurial suture).

Behavioral studies

The tapered/ledged beam apparatus is a skilled locomotor test, which has been previously shown to assess behavioral recovery without masking return of functional capacity through learned compensatory mechanisms (Kemp et al., 2010; Zhao et al., 2005). The animals were trained to cross a horizontally elevated tapered beam (100 cm high; 80 × 5 cm) for a period of 2 weeks prior to surgical intervention. Ten satisfactory runs were used for each animal at each time point, with a satisfactory run consisting of the animal traveling across the beam uninterrupted at a constant velocity. The rats' performance was video recorded and later analyzed in a frame-by-frame fashion at 60 Hz by a trained observer blinded to the experimental conditions. The number of times that an animal slipped off the ledge with their affected right hindlimb was recorded, and the number of slips was normalized to the total number of steps taken. Slips off the ledge were scored as a full slip (given a score of 1), or a half slip (given a score of 0.5) if the limb touched the side of the beam. A slip ratio (%) was calculated as the number of right hindlimb slips per total number of right hindlimb steps. Following surgery, the animals were tested at the first week post-surgery, and then at weeks 3, 5, and 8.

The horizontal ladder rung test has previously been used to assess return of skilled locomotor behavior following nerve injury in rats (Kemp et al., 2010). Animals were trained to cross a horizontally placed ladder for a period of 2 weeks prior to surgical intervention. The apparatus consisted of sidewalls made of clear acrylic glass (1 m long, 20 cm high), and metal rungs (3 mm diameter), which were inserted 1 cm from the bottom of the acrylic glass, and could be spaced 1 cm apart. During testing, an irregular pattern of the rungs was changed from trial to trial in order to prevent the animals from learning the spacing pattern (distance of the rungs varied from 1 to 3 cm). Ten satisfactory runs were used for each animal at each time point, with a satisfactory run consisting of the animal traveling across the beam uninterrupted at a constant velocity. A mirror was placed at a 45° angle below the ladder so that the rats could be video recorded with both a lateral and a ventral view. Each rat was video recorded and later analyzed frame-by-frame by a trained observer blinded to the experimental conditions. Steps with the right hindlimbs were scored as a correct or an incorrect step. Incorrect steps consisted of steps that involved a total miss of the rung or a deep slip from the rung, similar to a score of 0 or 1 in the scoring system of Metz and Whishaw (2002). A slip ratio (%) was then calculated as the number of right hindlimb slips per total number of right hindlimb steps. Following surgery, the animals were tested at the first week post-surgery, and then at weeks 3, 5, and 8.

Ground reaction forces (GRFs) are defined as the forces exerted by an animal's limbs on the ground during flat surface locomotion. GRFs can be measured to determine the contribution of each limb for weight support, propulsion, braking, and balance during locomotion. These forces have recently been shown to provide a direct measure, which objectively and sensitively measures the return of locomotor function following nerve injury in rats (Boyd et al., 2007; Howard et al., 2000; Kemp et al., 2010). The animals were trained to cross a flat surface runway for food reward. A force platform was placed level with the runway surface and was located in the middle of the runway, equidistant from each end. The platform (HE6X6-5, Advanced Mechanical Technology Inc., Watertown, MA; 10.5 × 11 cm) measured force in three orthogonal directions: vertical, fore-aft (braking and propulsive force), and medio-lateral. Ground reaction force data were collected at 1200 Hz. The animals were videotaped with four different cameras (Model LTC0510; Bosch Security Systems, Fairport, PA) at 60 Hz, placed approximately 90° from each other, to permit calculation of velocity of movement and for optional kinematic analysis (Webb et al., 2010). All GRF data were imported and filtered using Peak Motus software (Vicon, Denver, CO). GRF data were collected and analyzed from 5 acceptable runs for each left and right limb pair at each time point, and was used to provide average GRFs for each side of the body. Acceptable runs collected were those that consisted of the animals trotting at a constant velocity of 60–90 cm/sec (Kemp et al., 2010; Muir et al., 2007; Webb and Muir, 2004;). Trotting is a form of gait employed by rats, and involves the alternating pattern of diagonal limbs being placed on the ground. GRF data were exported as ASCII data and analyzed using custom written software (MatLab; The Mathworks, Inc., El Segundo, CA). Data for left and right limbs were kept separate for each rat, expressed as a proportion of body weight, and normalized to stride duration. Averaged GRF data from each rat were then used to calculate group GRF data. GRFs were collected from all animals after baseline training, and then at 2, 4, 6, and 9 weeks.

Variables of the GRF data examined statistically included both mean peak and mean impulse (area under the curve) for: (1) vertical, (2) fore-aft (braking and propulsion), and (3) medio-lateral forces of the left and right limb pairs.

Statistical analysis

Differences between groups were compared using two-tailed unpaired *t*-tests. Statistical significance was accepted at $p < 0.05$, with all results presented as the mean ± standard error of the mean (SEM).

Results

Macroscopic evaluation and histology of in vivo *experiments*

Initial comparison of the different *in vivo* nerve injuries were made by macroscopic and microscopic evaluation of the

injury zones at various time intervals for qualitative/descriptive purposes, and for selection of the most appropriate injury model for the behavioral component of the study that best resembled NIC features (Table 1). Macroscopically, the simple 30-sec jeweler's forceps crush injury sites were almost transparent immediately after the injury. Occasionally a small area of epineurial disruption was seen with the experimental NIC nerve injuries. Macroscopic evaluation of the injury zones at 5 days did not reveal noticeable differences between the simple crush and malleus nipper compressions with or without 50 g traction. Only minimal adhesion of the nerve to the surrounding tissue was noticed at all time points, and was similar in all injury techniques. At days 13, 21, and 65, very subtle fusiform enlargement of the injury zones could be appreciated in the malleus nipper with 50 g traction nerves, whereas the simple crush-injured nerves appeared to be of normal caliber (Fig. 2).

H&E preparations were not helpful at 5 and 13 days to differentiate between grades 2, 3, and 4 injuries, with nonspecific wallerian degeneration changes visible a millimeter or so proximal and all the way distal to all the injuries as expected. Masson's trichrome stain, which stains collagen blue, was more useful, especially to demonstrate disruption and deposition of connective tissue components (Fig. 3). The neurofilament immunostains were most helpful to demonstrate the regeneration morphology of the axons (Figs. 4–6).

The jeweler's forceps crush injuries showed wallerian degeneration distal to the inconspicuous injury zones. No disruption of the perineurium was seen or regeneration outside perineurial boundaries. Regeneration was organized, rapid, and already established up to the distal specimen at 5 days on neurofilament stains. No indication of neuroma formation was found at any time point (days 5, $n=1$; 13, $n=1$; 65, $n=5$), as expected (Fig. 5).

The specimens from jeweler's forceps crush injury with 50 g traction (days 5, $n=1$; 13, $n=1$) demonstrated minimal additional injury, with only minimal aberrant intrafascicular axonal regeneration, that was non-uniform towards one side of a few sections. There were also indications of focal perineurial breach on one side of some sections, with minimal extrafascicular regeneration on neurofilament stains (Fig. 4). These few injuries confirmed our suspicion from *ex vivo* pilot experiments, that this injury paradigm was not going to yield uniform and sufficiently severe injuries to pursue it further by adding more injuries to this group.

The malleus nipper-alone injuries (days 5, $n=4$; 13, $n=1$) also occasionally showed some areas of chaotic intrafascicular and extrafascicular regeneration, but this also appeared to be non-uniform. The majority of these injuries also appeared to conform to what is seen in crush injuries (Fig. 4). At day 5, neurofilament profiles distal to the injury were also more abundant than what was observed in the specimens in which the malleus nipper was combined with traction, suggesting more efficient regeneration and less severe injury. Generally, the 13-day time point did not yield useful additional histological information, and no more injuries were added to this time point. Initially, it was still unclear whether traction was necessary to optimize the injury severity, and therefore more injuries were added to this group for 5-day histology to assess this further.

In the group with malleus nipper injuries with 50 g traction (experimental NIC; days 5, $n=5$; 13, $n=1$; 21, $n=2$; 65, $n=6$), the most extensive and uniform neuroma formation was seen, with chaotic intrafascicular axonal regeneration spanning across the fascicles at the injury zones, and extrafascicular regeneration visible on both sides of the nerve sections (Figs. 5 and 6). Perineurial disruption was demonstrated most prominently at 5 days with both laminin and Masson's trichrome stains. Progressive intrafascicular and extrafascicular collagen deposition on Masson's trichrome stains was evident after 13 days (Fig. 3). Mini-fascicle formation within the epineurium was also visible at 65 days (Fig. 7). These features were evident in all 14 injured nerves examined after experimental NIC injuries with refined methods as described above.

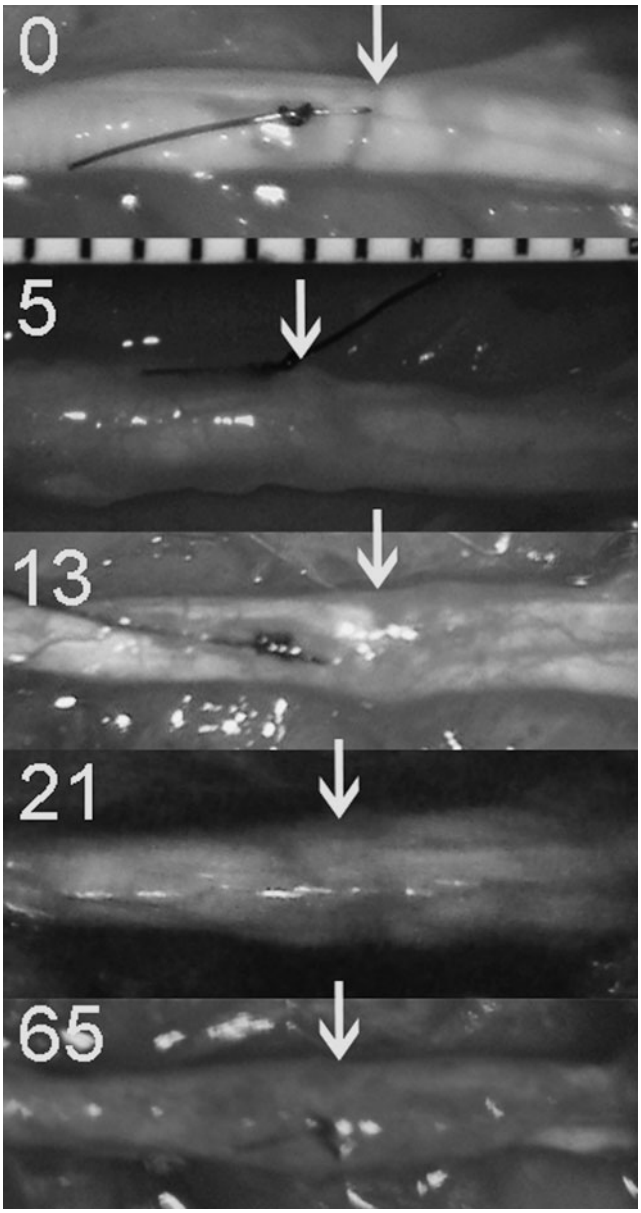

FIG. 2. *In situ* photos of the experimental neuromas in continuity injury zones at 0, 5, 13, 21, and 65 days post-injury demonstrate subtle focal fusiform enlargement after 13 days. The nerves are oriented proximal (left) to distal (right). Injuries were made just distal to the marking sutures and are indicated with arrows (millimeter scale visible).

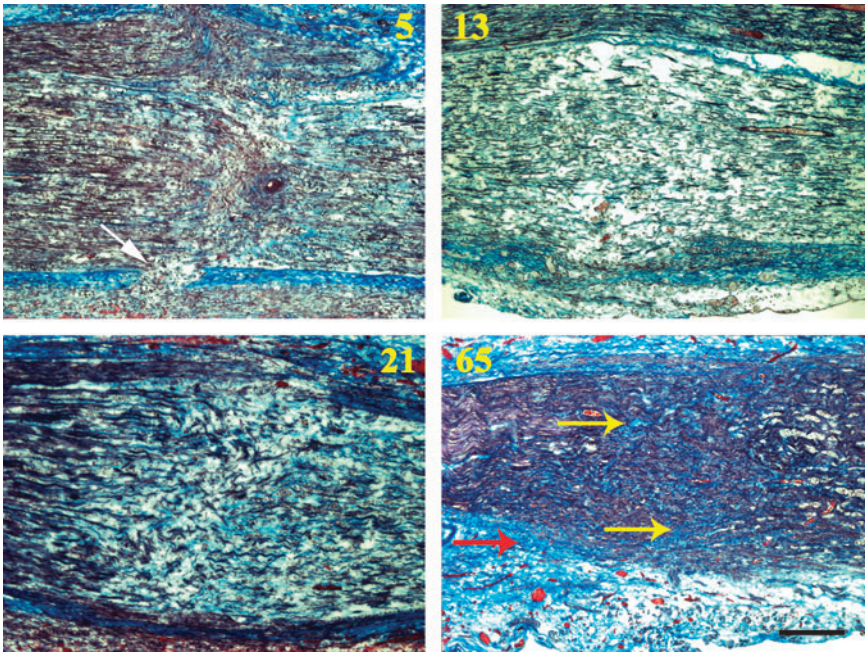

FIG. 3. Progressive intrafascicular (yellow arrows) and extrafascicular (red arrow) scar formation was demonstrated using Masson's trichrome stain within the experimental neuroma in continuity (malleus nipper with 50 g traction) injury zones. Collagen is stained blue. All figures are oriented proximal (left) to distal (right). The white arrow marks an area of perineurial disruption at the bottom of the 5-day image (days 5, 13, 21, and 65; scale bar = 250 μm). Color image is available online at www.liebertonline.com/neu

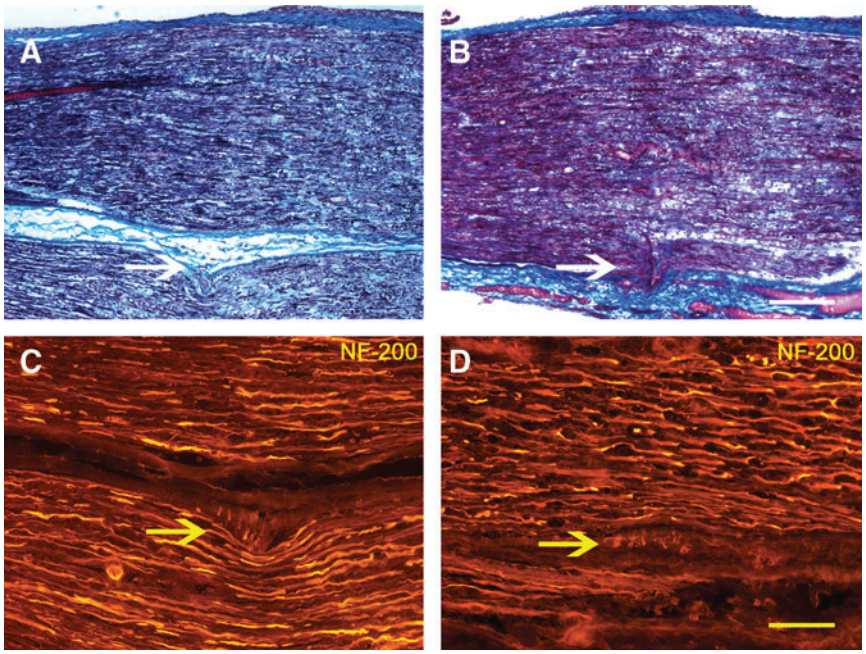

FIG. 4. Histology of crush injuries combined with 50 g traction and malleus nipper injuries without traction demonstrated only minimal signs of endoneurial and perineurial injury. The overall appearance of these injuries conformed to simple axonotmetic injuries. Comparison at 5 days of crush with traction Masson's trichrome (**A**), and neurofilament-200 immunostains (**C**), with malleus nipper compression without traction (**B** and **D**) injury zones that show findings similar to simple crush injury morphology. The white arrows point to perineurial disruption, and the yellow arrows to minimal aberrant axonal growth. All figures are oriented proximal (left) to distal (right; scale bar = 250 μm in **A** and **B**; scale bar = 100 μm in **C** and **D**). Color image is available online at www.liebertonline.com/neu

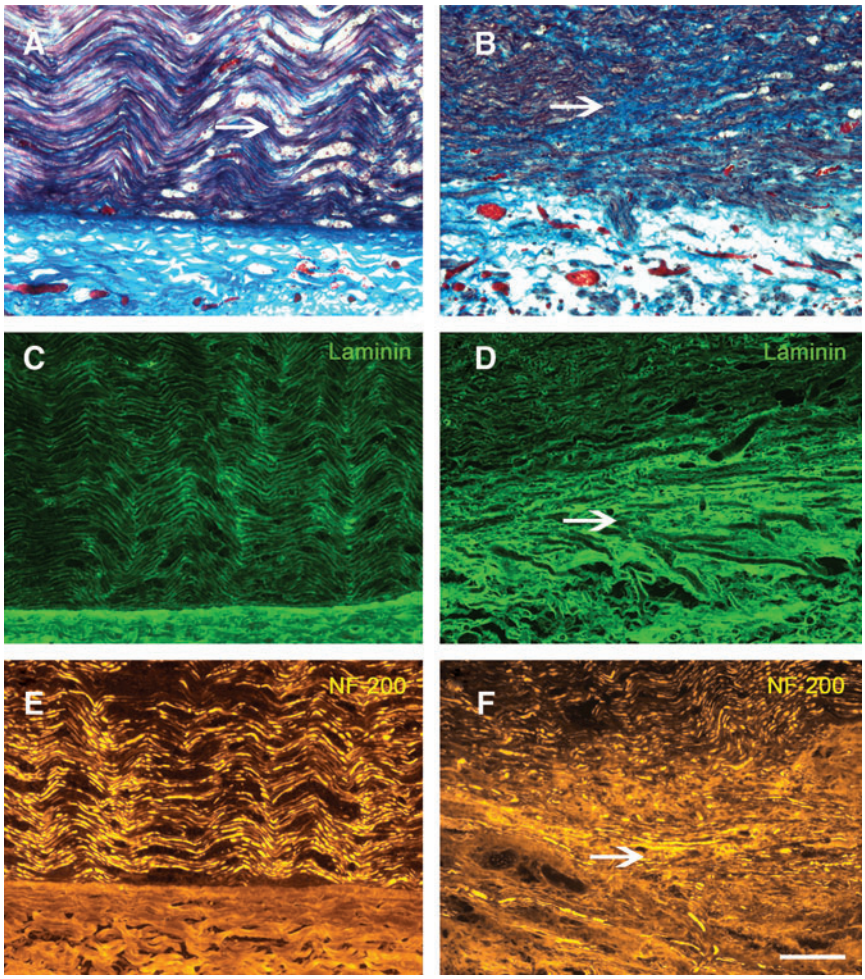

FIG. 5. At 65 days experimental neuroma in continuity (NIC) injuries (**B**, **D**, and **F**) were markedly different and in contrast to the crush injury (control) histology (**A**, **C**, and **E**). Masson's trichrome demonstrated remnants of wallerian degeneration in the crushed nerves (**A**), but prominent intrafascicular scarring in the NIC nerves (**B**). Laminin immunostains also demonstrated the distorted perineurial layer in experimental nerves (**D**). Aberrant extrafascicular axonal neurofilament-200 (NF-200) profiles in the NIC nerves (**E**) clearly contrast to the organized axonal regeneration seen after crush injuries (**E**). All figures are oriented proximal (left) to distal (right), with the periphery of the nerves at the bottom of the figures; the arrows point to the described pathology (scale bar = 100 μm). Color image is available online at www.liebertonline.com/neu

Histological observations at 5 days also suggest a regeneration delay, with relatively few neurofilament axon profiles visible distal to the injury zones in the experimental NIC injuries, compared to the abundant profiles seen in the simple crush injuries.

Pressure measurements

Forces exerted on a load cell were determined to illustrate the approximate and relative pressures employed in these injuries. The average maximal pressure exerted by the experimental malleus nipper was 182 MPa (range: 170.2–194.5 MPa) in SI units, which is perhaps more tangibly expressed as 18.56 kg force/mm^2 (range: 17.36–19.84 kg force/mm^2). The no. 5 jeweler's forceps average maximal pressure was 16.81 MPa (1.714 kg force/mm^2).

Behavioral results

Skilled locomotion tasks (tapered beam, ladder rung) and GRFs were used as functional outcome measures to compare experimental NIC injuries to simple crush injuries, which are widely employed in peripheral nerve research. Animals with successful NIC lesions were expected to fare significantly worse than those with crush injuries on behavioral tasks.

Skilled locomotion analysis. Both tapered beam and ladder rung slip ratios of animals with the experimental NIC injuries showed significantly less recovery compared to crush injuries up to 8 weeks (Fig. 8). Skilled locomotion (Fig. 8A) was first assessed through accurate placement of the right hindlimb on the tapered beam apparatus without slipping onto the adjacent lower ledge. Consistent with previous research, intact rats moved across the beam quickly and easily, and made very few slipping errors with a mean incidence of approximately 5% (Kemp et al., 2010). At the 1- and 3-week time points, both groups performed poorly, but at 5 weeks the crush-injury group started to show improvement of slip ratios. Eight weeks post-injury, the animals in the experimental group still did not show significant recovery of slip ratios compared to week 3 [$t(9) = 1.25$, $p > 0.05$]. In contrast, the

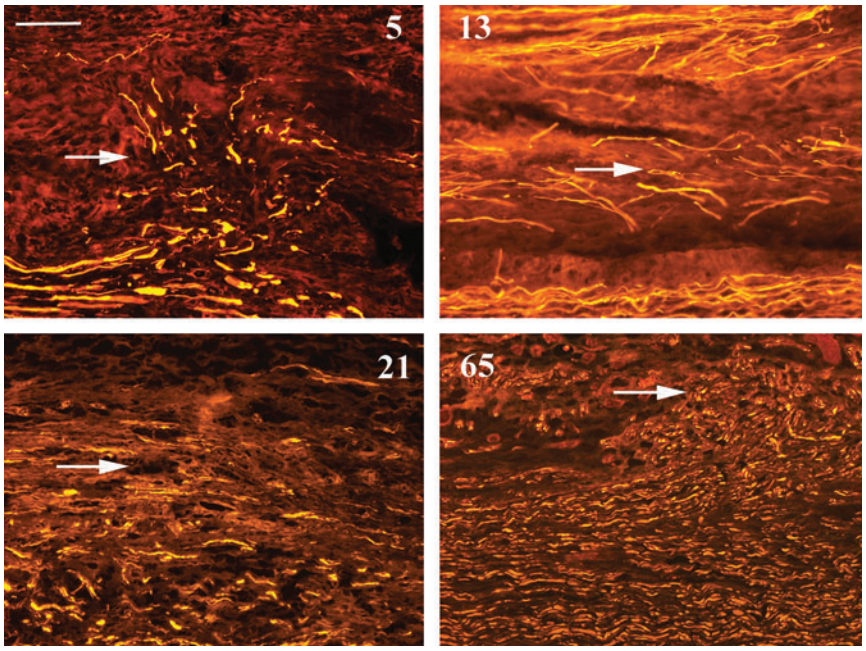

FIG. 6. At 5, 13, 21, and 65 days aberrant intrafascicular and extrafascicular axonal regeneration was demonstrated at the experimental neuroma in continuity injury zones. Extrafascicular regeneration is seen toward the top of these images, as shown by the arrows. All figures are oriented proximal (left) to distal (right), with the periphery of the nerves at the top of the figures (neurofilament-200 immunostain in yellow; scale bar = 100 μm). Color image is available online at www.liebertonline.com/neu

crush-injured group continued to show improvement, compared to week 3 [t (9) = 5.25, $p < 0.05$]. Five- and 8-week slip ratios showed statistically significant differences between the crush and experimental groups [t (9) = 7.25, $p < 0.05$]. Analysis of the ladder rung skilled locomotion task (Fig. 8B) demonstrated accurate placement of right hindlimbs on the rungs, with few slips in both groups at baseline (approximately 6%). Similar to the tapered beam results, both groups performed poorly at weeks 1 and 3, but the experimental group showed no statistically significant improvement in their injured limb

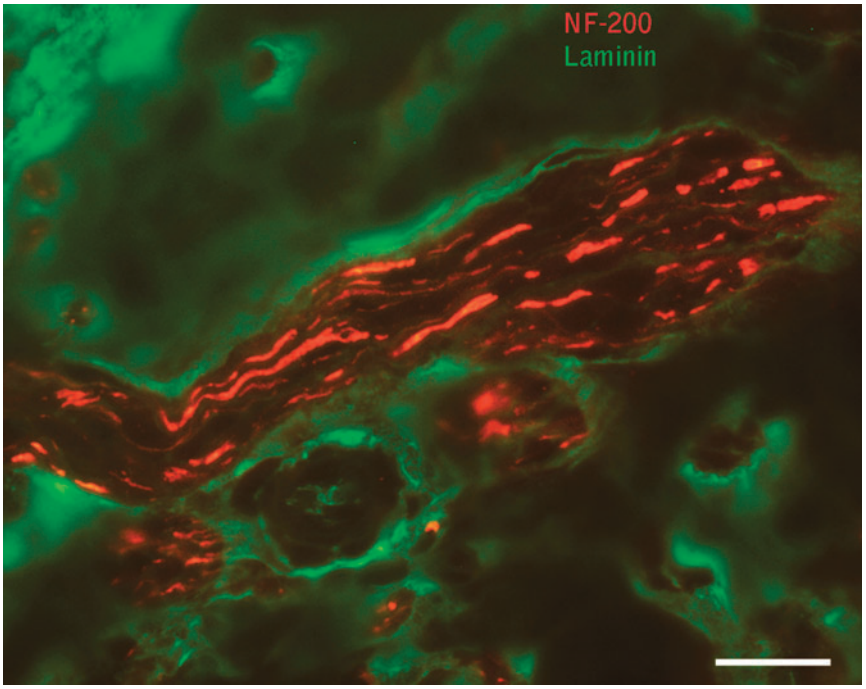

FIG. 7. Mini-fascicle formation was visible within the epineurium of experimental neuroma in continuity specimens as multiple small bundles of axons at 65 days (neurofilament-200 is red; laminin is green; scale bar = 20 μm). Color image is available online at www.liebertonline.com/neu

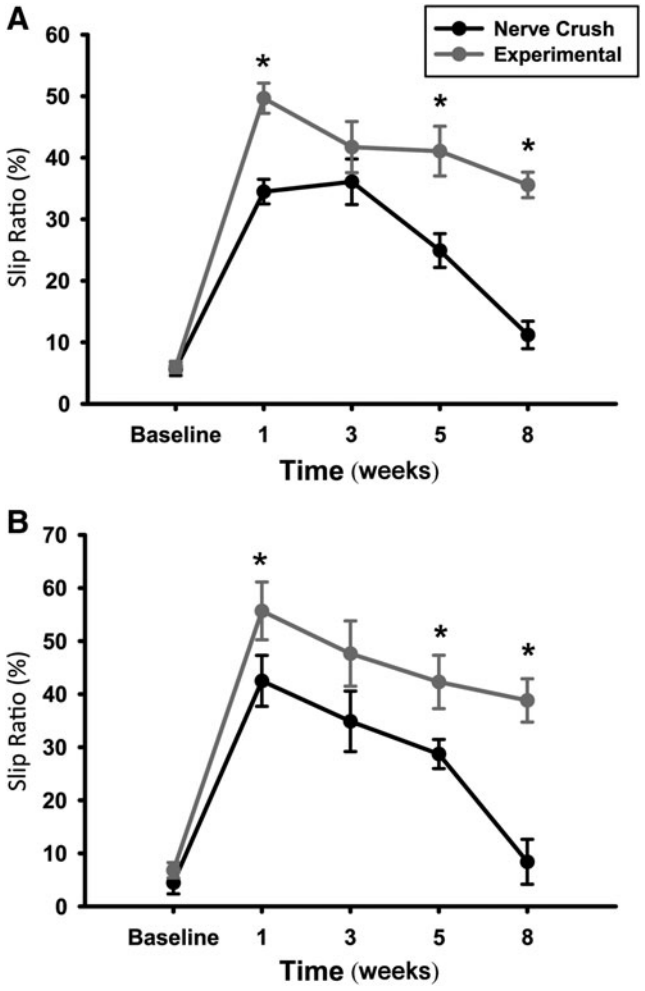

FIG. 8. Injured limb slip ratios of the experimental neuroma in continuity (NIC) animals ($n=6$) at 5 and 8 weeks post-injury, were significantly worse in the tapered beam (**A**) and ladder rung (**B**) skilled locomotion tasks compared to simple crush-injured ($n=5$) animals (*$p<00.05$). Note that crush-injured animals have returned close to baseline performance, whereas experimental NIC animals continued to exhibit slips in approximately 40% of injured hindlimb steps.

slip ratios from week 3 to week 8 [t (9) = 1.75, $p>0.05$]. The crush group slip ratios improved, with statistical significance seen between 3 and 8 weeks post-injury, as expected [t (9) = 5.77, $p<0.05$]. The experimental and crush group slip ratios also differed, with statistical significance seen at 5 and 8 weeks [t (9) = 12.89, $p<0.05$].

Ground reaction forces. As expected, maximal deficits in gait were demonstrated at the 2-week time point in both groups. At 4 weeks, the crush-injured group's vertical GRF patterns of their injured (right) side showed clear recovery towards baseline, and was statistically significantly different from that of the NIC experimental group for both forelimb [t (9) = 7.50, $p<0.05$], and hindlimb vertical forces [t (9) = 6.25, $p<0.05$; Fig. 9A and B). Experimental NIC animals displayed a far lesser degree of recovery at this time-point, with left (uninjured) side forelimb and hindlimb vertical forces increased to compensate for right-sided deficits (data not shown). This may indicate a relative delay in muscle re-innervation in the experimental group due to regeneration impairment at the injury site. Both left- and right-side crush and experimental NIC vertical GRF patterns recovered towards baseline at 9 weeks, although right (injured) hindlimb forces did not fully return to baseline values in both groups. Interestingly, this does not reflect the persistent sensorimotor coordination deficits demonstrated on the skilled locomotion tasks.

At 9 weeks, forelimb vertical forces returned to baseline levels for both groups. However, hindlimb vertical forces were statistically significantly lower for both the crush and NIC groups compared to their original baseline values (Fig. 9C and D). The animals in the crush-injured group improved only modestly from 4 to 9 weeks. However, hindlimb vertical forces in the NIC group improved significantly during this time period [t (9) = 5.68, $p<0.05$; Fig. 9D]. At 9 weeks, right forelimb and hindlimb fore-aft force patterns of both the crush-injured and NIC group were not significantly different from baseline values (Fig. 9E and F). Interestingly, animals in the NIC group used their left (uninjured side) forelimbs to brake to a significantly greater extent than their right forelimbs, compared to baseline values [t (9) = 5.50, $p<0.05$; data not shown].

Discussion

Neuroma models

Song and associates (2006) proposed a NIC model in rabbits. They excised a 15-mm segment of the lateral peroneal fascicle, and observed histological features of neuroma formation in close relation with the undisrupted medial peroneal fascicle. Kerns and colleagues (2005) also attempted to recreate an NIC model in rats with 8-mm partial tibial neurectomy with limited success. We consider these models to be more closely related to side-neuroma, which occur in an eccentric fashion on one side of the nerve and may be relevant to partial transection injuries (Midha, 2008). With crush and transection of the common peroneal nerve, followed by repair with the interposition of muscle aponeurosis, Tomita and colleagues (2007) reproduced histological features of NIC, although they initially induced a complete transection injury.

Moradzadeh and co-workers (2010) recently published an electro-thermal injury model of the rat sciatic nerve. With bipolar electrocautery, they reproduced functional deficits in accord with Sunderland grade 3 injuries. Histologically, electro-thermal injuries were reported to be similar to crush injuries. The reported focal edema at the injury zones at 21 days, and retarded nerve regeneration (compared to crush injuries), are consistent with our observations. Walking track analysis showed minimal recovery up to 6 weeks after electro-thermal injuries. Hnatuk and associates (1998) applied similar currents to the rat tibial nerve, and observed disorganized intra- and extrafascicular regenerating fibers, suggesting Sunderland grade 4 injuries. They also demonstrated partial recovery of plantaris and soleus muscle twitch and titanic forces up to 8 weeks post-injury. The physical forces employed in their models are different from those responsible for the vast majority of nerve injuries encountered in clinical practice, which may limit their general utility as NIC models. Others have suggested that diathermy application limits the degree of neuroma formation (Tay et al., 2005).

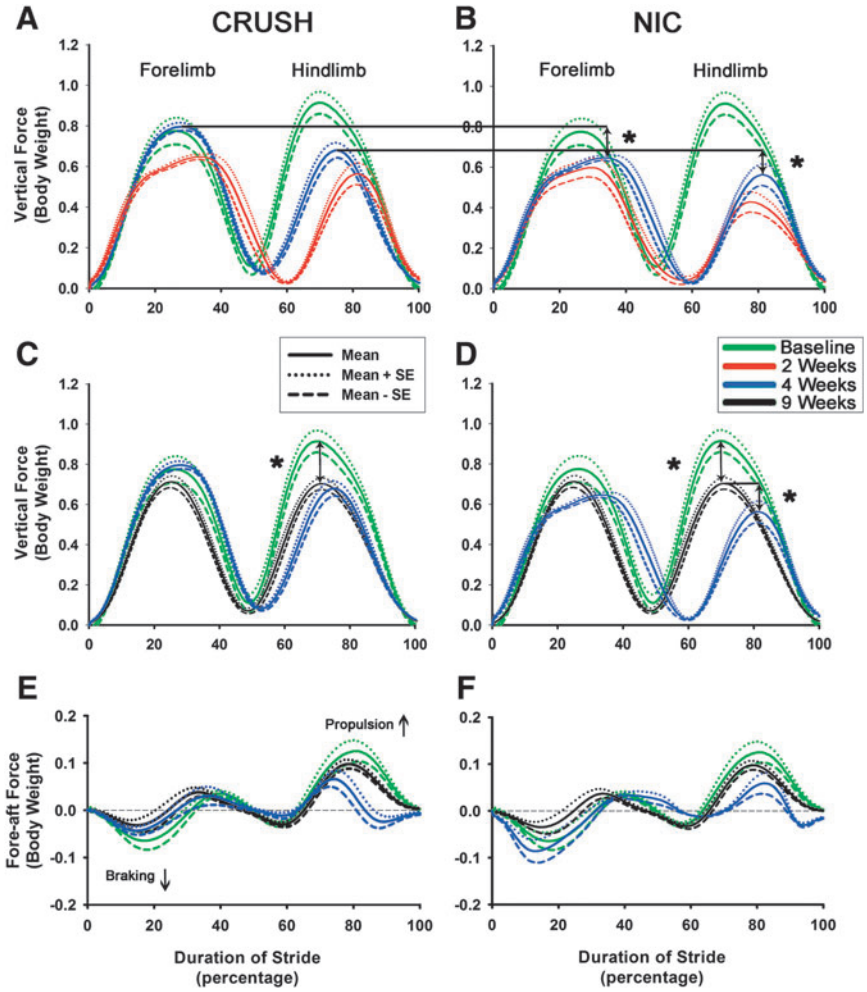

FIG. 9. Right side vertical and fore-aft ground reaction forces at baseline (green), 2 weeks (red), and 4 weeks (blue; **A** and **B**), and baseline, 4 and 9 weeks (black) post-surgery (**C**–**F**) superimposed. The peak vertical forces exerted by forelimbs and hindlimbs on the injured side of the experimental neuroma in continuity (NIC) group at 4 weeks (blue traces) demonstrated delayed recovery, with statistically significant differences compared to the crush group at this time point (**A** and **B**). Although crush and experimental NIC vertical and fore-aft forces at 9 weeks (black traces in **C**–**F**) were not significantly different between groups, peak vertical forces exerted by injured hindlimbs of both groups had not completely returned to baseline values (black and green traces in **C** and **D**). At 4 weeks the crush group peak vertical forces had already plateaued close to 9-week values, but the experimental NIC group still showed statistically significant recovery in the injured hindlimbs up to 9 weeks (blue and black traces in **D**). Forces are normalized to body weight. The solid lines represent the mean for each group, while the dotted and dashed lines represent the mean ± standard error of the mean. Rodents use their forelimbs for braking (downward defection), and their hindlimbs for propulsion (upward deflection) during a trotting gait. Double-ended arrows represent the differences between the indicated force traces (*$p < 0.05$). Color image is available online at www.liebertonline.com/neu

Mavrogenis and colleagues created an unpublished animal model of NIC by the 10-sec application of a straight hemostat in peripheral nerves of rats, with histological features of neuroma formation (Mavrogenis et al., 2008). We have also found that partial disruption of the perineurium and endoneurium may be seen with injuries by similar instruments. These are often non-uniform and hard to consistently reproduce. We speculate that this is the result of shear forces, since the pressure exerted by these instruments is close to that of a jeweler's forceps.

The traction injury model described by Spiegel and colleagues (1993), with rat sciatic nerve rupture but preservation of gross nerve continuity in the plastic zone, also technically resulted in NIC formation histologically, with demonstrable deficits on walking track analysis up to 8 weeks. Traction forces around 600 g were needed to produce these injuries, and the amount of traction needed to rupture the nerves was unpredictable, making it difficult to standardize the injury. Specialized equipment was required to stretch the nerves at a constant rate. The amount of injury inflicted at more remote sites from the epineurial rupture zone is undetermined, making it difficult to isolate the injury for experimental purposes (Haftek, 1970; Zachary et al., 1989).

Tools and forces

The pressure exerted by our experimental malleus nipper was approximately 10-fold that of the jeweler's forceps. Because of the technical difficulties in measuring these forces, we can with reasonable certainty report the relative pressure

difference between these instruments as determined by the described technique, but the precise point pressure may not be entirely accurate. We still include these findings to illustrate the magnitude of compression forces involved in these injuries. The high range pressures employed in standardized crush injury models (up to 20.43 and 22.5 MPa) to induce adequate crush injuries, compare well to our measured jeweler's forceps pressure (Beer et al., 2001; Ronchi et al., 2010). Applied pressures will also vary depending on animal-to-animal variation in nerve size.

When applying the compression force with the malleus nipper, it is important to position the nerve at the same approximate portion of the blades every time, to ensure compression of the whole nerve with consistent pressure. Other instruments (e.g., diagonal cutting pliers) that can exert high compression forces may also recreate similar injuries. The unique feature of the malleus nipper is that there is a definite endpoint to the maximal amount of pressure that can be exerted on the nerve by the particular instrument. This internal standard helps to simplify the reproducibility of the injury, without the need for force measurements for every injury. Not applying the maximal closing force with our experimental malleus nipper resulted mostly in histological grade 2 injuries, with variable and minimal endoneurial and perineurial disruption, even when combined with the 50-g traction force ($n = 4$; data not shown). The malleus nipper used in this experiment was not new, and most of the fine serrations on the blades were worn down and nearly absent. It may be necessary to carefully file down the blade serrations of a new instrument to avoid non-homogenous pressure with sparing of nerve portions (Beer et al., 2001). No amount of visible lateral play between the blades should be present. This creates the potential for significant shear forces that are difficult to control and result in unpredictable nerve transection.

The traction force of 50 g was arbitrarily selected and could arguably have been 75 or 100 g instead. Traction of 75 g elevates the hindlimb, and some counter-traction is needed to stabilize the limb and target injury site. It is plausible that even jeweler's forceps compression (crush) forces combined with a much higher traction force may lead to a similar NIC injury pattern. However, this makes traction injury distant from the crush zone more likely and difficult to determine *in vivo* (Haftek, 1970). The selected 50-g traction is less than a tenth of the average traction required to disrupt the rat sciatic nerve (Spiegel et al., 1993). Spiegel and colleagues (1993) also demonstrated that in animals in which traction was around 600 g did not result in nerve disruption, and the sciatic functional index deficits recovered to baseline within 2 weeks. For this reason we did not include a 50-g-traction-alone group, since only minimal transient deficits (if any) are expected from this degree of sciatic nerve traction. Sunderland proposed that nerve traction injuries result in failure of the connective tissue elements in a similar sequence as his grading system (endo- then peri- and lastly epineurial rupture; Sunderland, 1978). Haftek and associates (1970), and Spiegel and colleagues (1993), have alternatively presented evidence that this sequence may in fact be the reverse of that which Sunderland proposed. It would furthermore be logical for the large amount of thick, longitudinally-oriented collagen fibrils in the epineurium to fail before the nerve fibers, indicating that they do in fact offer meaningful shielding to the endoneurium from excessive traction. Longitudinally arranged peri- and endoneurial collagen and perineurial elastin fibers are likely responsible for the redundant nerve fiber length in the relaxed nerve, observed as the bands of Fontana, and these provide needed slack and thus prevent failure when the nerve is exposed to moderate traction within the elastic zone (Sunderland, 1978). This supports our findings that the peri- and endoneurium, protected by the epineurium against pure traction within its capacity, fail when additional compression is applied beyond a critical threshold. The tension makes the normally resilient endo- and perineurium more vulnerable to failure when under additional stress (compression). We suspect that the traction force may not be essential to recreate adequate NIC features, and that even higher compression forces alone may result in a similar injury pattern. We argue that the small traction force is easy to add, and that it likely expands the experimental NIC window between simple crush (grade 2) and nerve transection (grade 5), to accommodate some inter-animal (e.g., nerve size) and other technical variations. We are currently working on defining these thresholds.

Selection of time intervals

The 5-day time point was selected to allow for adequate regeneration past the injury zone in crush injuries, and to detect early aberrant regeneration in the NIC injuries. This was found to be a practical and useful interval to detect differences between the injuries in pilot experiments. The 13- and 21-day histological intervals were chosen for lesion descriptive purposes only, and therefore fewer injuries were evaluated at these time points. Sixty-five-day histology was obtained at termination of the behavioral component of the study to confirm successful neuroma formation in the experimental NIC group. The duration of behavioral assessment was set at 8–9 weeks on the basis of recent experiments in our lab that showed plateauing of the skilled locomotion and GRF data from weeks 7–11 after sciatic nerve transection with direct repair (Kemp et al., 2011).

Histological evaluation

It was our goal to recreate as extensive an injury as possible, but still leave the majority of the epineurium in gross continuity. Clinically there are often mixed degrees and combinations of axonotmesis and perineurial and endoneurial disruption (Mackinnon, 1989). A reproducible injury within this spectrum should be helpful for research purposes. The degree and extent of neuroma formation would be hard to quantify objectively, but their presence is relatively easy to recognize, especially at later time points. Intra-epineurial axonal profiles originating from the severed small cutaneous branch close to the injury site should not be confused with the extrafascicular regeneration seen in grade 4 injuries. To avoid this misinterpretation, we severed this cutaneous branch as far as possible from its origin at the sciatic nerve, so that its inevitable regeneration is removed from the experimental injury zone. We found that proper longitudinal sections through the neuroma are essential to accurately evaluate the histological extent of the injury. In addition, the 5-day neurofilament immunofluorescence stains are most useful for early demonstration of extrafascicular axonal profiles, implying both the endo- and perineurial disruption required for grade 4 injuries.

Behavioral data

GRF results showed only subtle gait pattern differences between the groups at 9 weeks, and a relative lag in recovery of the experimental NIC group. The skilled locomotion tasks, however, demonstrate the relative deficits much more clearly and are less labor intensive to perform. Commonly used tools for behavioral analysis after peripheral nerve injuries like walking track analysis have their own inherent disadvantages, and may not be sensitive enough to detect the differences demonstrated by the skilled locomotion tasks and GRFs (Sarikcioglu et al., 2009). Profound deficits clinically associated with NIC were not observed in this study, or in the electro-thermal NIC models. The relatively short regeneration distances to the rat end organs may largely explain this, which is an inherent shortcoming of all rodent nerve injury models. For experimental purposes, it is advantageous to demonstrate some recovery within a reasonable period, in order to measure the functional effects of intervention strategies more clearly.

Shortcomings and future studies

We did not have sham-surgery (positive control) or nerve transection (negative control) groups to compare the behavioral outcomes within this study. During several previous studies we have learned that sham-surgery results are very similar over a wide range of time to the baseline behavioral data collected (Kemp et al., 2010,2011). Our results are based on the injuries induced by the same malleus nipper. We are in the process of evaluating injuries induced by other malleus nippers and the maximal pressures they exert. This may help to define the threshold forces needed to recreate NIC. Two of the 14 experimental injuries were inflicted by a different surgeon, using the same experimental instruments and methods. We found 100% histological reproducibility of grade 4 features with these methods. In the crush-injury model, the specific instrument and even duration of compression do not seem to make that much difference, as long as the same operator uses the same instruments and methods to conduct a certain experiment. Groups can then be compared with more confidence (Bridge et al., 1994). It therefore remains important that pilot studies be conducted first by any lab wishing to use this model, to confirm that the desired injury can be reproduced with their own unique instruments and expertise. This injury model was developed for the sciatic nerve, and the methods may need to be modified for nerves of different caliber and location. Retrograde labeling studies are in progress to further characterize this injury model in terms of the axonal misdirection. Later behavioral assessments, especially with skilled locomotion tasks, should be employed in future studies, which may show more recovery of NIC injuries over time.

Conclusion

We have demonstrated histological features and poor functional recovery consistent with NIC formation in a rodent model. The injury mechanism employed combines traction and compression forces akin to the physical forces at play in the majority of clinical nerve injuries. This relatively simple model may serve as a useful tool to help diagnose NIC earlier, and to develop intervention strategies to improve patient outcomes. Current work in our laboratory is further examining and defining the necessary threshold forces more clearly.

Acknowledgments

The authors are indebted to Dr. Christopher Hunter (PhD, MacCaig Institute for Bone and Joint Health, University of Calgary), for technical assistance and guidance with compression force determinations. Also, special thanks are due to Joanne Forden, for her help with the animal care and staining of the histological sections. This research was supported in part by funding from the Canadian Institute for Health Research Regenerative Medicine and Nanomedicine Group grant RMF-82496.

Author Disclosure Statement

No competing financial interests exist.

References

Beer, G.M., Steurer, J., and Meyer, V.E. (2001). Standardizing nerve crushes with a non-serrated clamp. J. Reconstr. Microsurg. 17, 531–534.

Bridge, P.M., Ball, D.J., Mackinnon, S.E., Nakao, Y., Brandt, K., Hunter, D.A., and Hertl, C. (1994). Nerve crush injuries—a model for axonotmesis. Exp. Neurol. 127, 284–290.

Boyd, B.S., Puttlitz, C., Noble-Haeusslein, L.J., John, C.M., Trivedi, A., and Topp, K.S. (2007). Deviations in gait pattern in experimental models of hindlimb paresis shown by a novel pressure mapping system. J. Neurosci. Res. 85, 2272–2283.

Burger, P.C., Scheithauer, E.W., and Vogel, F.S. (eds). (2002). The peripheral nervous system, in: *Surgical Pathology of the Nervous System and Its Coverings*, 4th ed. Churchill Livingstone: New York, pps. 585–587.

Chen, L., Gao, S.C., Gu, Y.D., Hu, S.N., Xu, L., and Huang, Y.G. (2008). Histopathologic study of the neuroma-in-continuity in obstetric brachial plexus palsy. Plast. Reconstr. Surg. 121, 2046–2054.

Fu, S.Y., and Gordon, T. (1995a). Contributing factors to poor functional recovery after delayed nerve repair: prolonged axotomy. J. Neurosci. 15, 3876–3885.

Fu, S.Y., and Gordon, T. (1995b). Contributing factors to poor functional recovery after delayed nerve repair: prolonged denervation. J. Neurosci. 15, 3886–3895.

Furey, M.J., Midha, R., Xu, Q.G., Belkas, J., and Gordon, T. (2007). Prolonged target deprivation reduces the capacity of injured motoneurons to regenerate. Neurosurgery 60, 723–732.

Haftek, J. (1970). Stretch injury of peripheral nerve. Acute effects of stretching on rabbit nerve. J. Bone Joint Surg. Br. 52, 354–365.

Hnatuk, L.A., Li, K.T., Carvalho, A.J., Freeman, J.L., Bilbao, J.M., and McKee, N.H. (1998). The effect of bipolar electrocautery on peripheral nerves. Plast. Reconstr. Surg. 101, 1867–1874.

Howard, C.S., Blakeney, D.C., Medige, J., Moy, O.J., and Peimer, C.A. (2000). Functional assessment in the rat by ground reaction forces. J. Biomech. 33, 751–757.

Kemp, S.W., Alant, J., Walsh, S.K., Webb, A.A., and Midha, R. (2010). Behavioural and anatomical analysis of selective tibial nerve branch transfer to the deep peroneal nerve in the rat. Eur. J. Neurosci. 31, 1074–1090.

Kemp, S.W., Webb, A.A., Dhaliwal, S., Syed, S., Walsh, S.K., and Midha, R. (2011). Dose and duration of nerve growth factor (NGF) administration determine the extent of behavioral recovery following peripheral nerve injury in the rat. Exp. Neurol. 229, 460–470.

Kerns, J.M., Sladek, E.H., Malushte, T.S., Bach, H., Elhassan, B., Kitidumrongsook, P., Kroin, J.S., Shott, S., Gantsoudes, G., and Gonzalez, M.H. (2005). End-to-side nerve grafting of the tibial nerve to bridge a neuroma-in-continuity. Microsurgery 25, 155–164.

Mackinnon, S.E. (1989). New directions in peripheral nerve surgery. Ann. Plast. Surg. 22, 257–273.

Mavrogenis, A.F., Pavlakis, K., Stamatoukou, A., Papagelopoulos, P.J., Theoharis, S., Zoubos, A.B., Zhang, Z., and Soucacos, P.N. (2008). Current treatment concepts for neuroma-in-continuity. Injury 39, S43–S48.

Metz, G.A., and Whishaw, I.Q. (2002). Cortical and subcortical lesions impair skilled walking in the ladder rung walking test: a new task to evaluate fore- and hindlimb stepping, placing, and co-ordination. J. Neurosci. Methods 115, 169–179.

Midha, R. (1997). Epidemiology of brachial plexus injuries in a multitrauma population. Neurosurgery 40, 1182–1188.

Midha, R. (2008). Mechanisms and pathology of injury, in: D.H. Kim, R. Midha, J.A. Murovic, and R.J. Spinner (eds). *Kline and Hudson's Nerve Injuries: Operative Results for Major Nerve Injuries, Entrapments and tumors*. Philadelphia: Saunders Elsevier, pps. 23–27.

Moradzadeh, A., Brenner, M.J., Whitlock, E.L., Tong, A.Y., Luciano, J.P., Hunter, D.A., Myckatyn, T.M., and Mackinnon, S.E. (2010). Bipolar electrocautery: A rodent model of Sunderland third-degree nerve injury. Arch. Facial Plast. Surg. 12, 40–47.

Muir, G.D., Webb, A.A., Kanagal, S., and Taylor, L. (2007). Dorsolateral cervical spinal injury differentially affects forelimb and hindlimb action in rats. Eur. J. Neurosci. 25, 1501–1510.

Ronchi, G., Raimondo, S., Varejão, A.S., Tos, P., Perroteau, I., and Geuna, S. (2010). Standardized crush injury of the mouse median nerve. J. Neurosci. Methods 188, 71–75.

Sarikcioglu, L., Demirel, B.M., and Utuk, A. (2009). Walking track analysis: an assessment method for functional recovery after sciatic nerve injury in the rat. Folia Morphol. (Warsz.) 68, 1–7.

Seddon, H.J. (1943). Three types of nerve injury. Brain 66, 237–288.

Song, C., Zhang, F., Zhang, J., Mustain, W.C., Chen, M.B., Chen, T., and Lineaweaver, W.C. (2006). Neuroma-in-continuity model in rabbits. Ann. Plast. Surg. 57, 317–322.

Spiegel, D.A., Seaber, A.V., Chen, L.E., and Urbaniak, J.R. (1993). Recovery following stretch injury to the sciatic nerve of the rat: An in-vivo study. J. Reconstr. Microsurg. 9, 69–74.

Sunderland, S. (1951). A classification of peripheral nerve injuries producing loss of function. Brain 74, 491–516.

Sunderland, S. (1978). *Nerves and Nerve Injuries,* 2nd *ed*. Churchill Livingstone: Edinburgh, pps. 38–45 and 151–156.

Tay, S.C., Teoh, L.C., Yong, F.C., and Tan, S.H. (2005). The prevention of neuroma formation by diathermy: An experimental study in the rat common peroneal nerve. Ann. Acad. Med. Singapore 34, 362–368.

Tomita, K., Kubo, T., Matsuda, K., Fujiwara, T., Kawai, K., Masuoka, T., Yano, K., and Hosokawa, K. (2007). Nerve bypass grafting for the treatment of neuroma-in-continuity: an experimental study on the rat. J. Reconstr. Microsurg. 23, 163–171.

Tos, P., Ronchi, G., Papalia, I., Sallen, V., Legagneux, J., Geuna, S., and Giacobini-Robecchi, M.G. (2009). Chapter 4: methods and protocols in peripheral nerve regeneration experimental research: part 1—experimental models. Int. Rev. Neurobiol. 87, 47–79.

Webb, A.A., and Muir, G.D. (2004). Course of motor recovery following ventrolateral spinal cord injury in the rat. Behav. Brain Res. 155, 55–65.

Webb, A.A., Kerr, B., Neville, T., Ngan, S., and Assem, H. (2010). Kinematics and ground reaction force determination: A demonstration quantifying locomotor abilities of young adult, middle-aged, and geriatric rats. JoVE http://www.jove.com/index/Details.stp?ID=2138

Zachary, L.S., Dellon, A.L., and Seiler, W.A. 4th. (1989). Relationship of intraneural damage in the rat sciatic nerve to the mechanism of injury. J. Reconstr. Microsurg. 5, 137–140.

Zhao, C.S., Puurunen, K., Schallert, T., Sivenius, J., and Jolkkonen, J. (2005). Behavioral effects of photothrombotic ischemic cortical injury in aged rats treated with the sedative-hypnotic GABAergic drug zopiclone. Behav. Brain Res. 160, 260–266.

Address correspondence to:
Jacob Daniel de Villiers Alant, MBChB, MMed, FRCS(C)
Foothills Medical Centre
Clinical Neurosciences
1403-29 Street NW
T2N 2T9, Alberta, Canada

E-mail: japiealant@hotmail.com